Journal of Power Sources 247 (2014) 721–728

Contents lists available at ScienceDirect

Journal of Power Sources

journal homepage: www.elsevier.com/locate/jpowsour

Improved electrochemical performance of spinel $LiMn_2O_4$ in situ coated with graphene-like membrane

Haitao Zhuo [a, b], Shuang Wan [a], Chuanxin He [a], Qianling Zhang [a], Cuihua Li [a], Dayong Gui [a], Caizhen Zhu [a], Hanben Niu [b], Jianhong Liu [a, *]

[a] Shenzhen Key Laboratory of Functional Polymer, College of Chemistry and Chemical Engineering, Shenzhen University, Shenzhen 518060, PR China
[b] Key Laboratory of Optoelectronic Devices and Systems of Education Ministry and Guangdong Province, Institute of Optoelectronics, Shenzhen University, Shenzhen 518060, PR China

HIGHLIGHTS

- Spinel $LiMn_2O_4$ in-situ coated with graphene-like membrane is prepared successfully.
- Graphene-like membrane is coated on surface of particle, without affecting crystal structure.
- Graphene-like membrane improves the electrochemistry performance of spinel $LiMn_2O_4$.
- Graphene-like membrane does not influence the insertion and desertion of Li^+.
- Improved electrochemical performance is attributed to in-situ coating of graphene-like membrane.

GRAPHICAL ABSTRACT

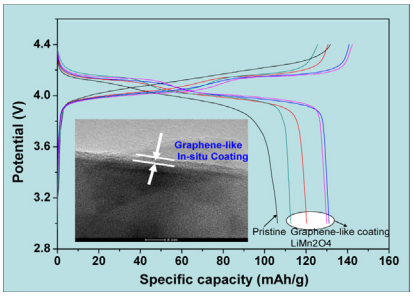

ARTICLE INFO

Article history:
Received 17 July 2013
Received in revised form
27 August 2013
Accepted 2 September 2013
Available online 11 September 2013

Keywords:
Spinel lithium manganese oxide
Graphene
Lithium-ion batteries
Coating
Liquid-polyacrylonitrile

ABSTRACT

In recent years, modifying cathode materials' surfaces become a popular pursuit. This paper reveals a novel spinel $LiMn_2O_4$ in situ coated with graphene-like membrane prepared using liquid-polyacrylonitrile (LPAN) as the carbon source. The structure and electrochemical performance of graphene-like membrane-coated spinel $LiMn_2O_4$ are investigated systematically. The membrane has a typical graphene-like layer carbon structure that can be applied the $LiMn_2O_4$ particles' surfaces in situ without affecting their crystal structure. Moreover, the graphene-like membrane helps to increase the particle size. The electrochemical performance reveals that coating the graphene-like membrane in situ significantly improves the discharge capacity and cycling stability of the spinel $LiMn_2O_4$. In particular, the spinel $LiMn_2O_4$ coated with a calcined 20 wt% LPAN graphene-like membrane in situ reached 131.1 mAh g^{-1} at room temperature, and up to 96% capacity is retained after 50 cycles at 0.1 C. The cyclic voltammetry and electrochemical impedance spectra analyses indicate that the graphene-like membrane does not influence the insertion or desertion of Li^+. The improved electrochemical performance is attributed to the decreased manganese dissolution in the electrolyte and the smaller charge transfer resistance generated by the graphene-like membrane coating.

1. Introduction

Spinel $LiMn_2O_4$ cathode materials are among the most promising cathode materials used in rechargeable lithium-ion batteries

* Corresponding author. Tel./fax: +86 755 26536141.
E-mail addresses: haitaozhuo@yahoo.com.cn (H. Zhuo), liujh@szu.edu.cn (J. Liu).

0378-7753/$ – see front matter © 2013 Elsevier B.V. All rights reserved.
http://dx.doi.org/10.1016/j.jpowsour.2013.09.007

(LIB) due to their low cost, fast charge–discharge reactions, high coulombic efficiency and non-toxicity compared to the $LiCoO_2$ cathode materials currently used [1–3]. However, the common spinel $LiMn_2O_4$ exhibits poor cycling behaviour because its capacity decreases. The factors might influencing performance include the dissolution of Mn^{2+}, the Jahn–Teller distortion of Mn^{3+} and electrolyte solution decomposition on the electrode [1]. In addition to modifying the preparation techniques and doping [4,5], surface modification improves the discharge capacity and the capacity retention of spinel $LiMn_2O_4$. Because the treating the spinel $LiMn_2O_4$ surfaces reduces the surface area, the side reactions between the electrode and electrolyte, as well as the Mn dissolution, decrease during cycling.

In recent years, modifying cathode materials' surfaces has become a popular pursuit among academic and industrial scientists. Numerous investigations have utilised surface modification to improve the electrochemical performance of spinel $LiMn_2O_4$ [6,7]. The reported surface coatings include oxides, metal phosphates, metals, electrode materials, fluoride materials, carbon materials and other novel materials [1]. In particular, the carbon coating enhances the electrical conductivity of metal oxides and increases their ability to absorb organic molecules [1,6,7]. For example, Han et al. utilised a novel soft chemical route to apply a carbon coating to spinel $LiMn_2O_4$ electrode materials; the carbon coating improved the electrode performance due to increased grain connectivity and/or by protecting the manganese oxide from chemical corrosion [8]. Akkisetty et al. reported a carbon-coated Li_2MnSiO_4/C composite synthesised in situ using a nanocomposite gel precursor alongside a carbon source (starch). The carbon coating facilitated electron movement, and the cathode materials demonstrated outstanding initial charge and discharge capacities (330 and 195 mAh g^{-1}, respectively) at 0.05 C [9]. Most recently, Tang et al. generated a novel $LiMn_2O_4$ material with small amounts of enwrapped carbon nanotube (CNT) segments. They reported the $LiMn_2O_4$/CNT composite cathode materials exhibited excellent high-rate capability in an aqueous electrolyte [10]. Therefore, carbon coating is an effective method for improving the discharge capacity and the capacity retention of spinel $LiMn_2O_4$.

Graphene is another promising carbon source due to its outstanding electronic behaviours, amazing mechanical properties and high surface area and has become more popular in recent years [11]. The cycling stability and the rate performance may be improved when electrode materials are coated or wrapped with graphene [12]. To date, many cathode materials, including $LiFePO_4$/C composite [13], thin $LiMnPO_4$ nanoplates [14], $Li_3V_2(PO_4)_3$ [15], $LiFePO_4$ [16] and $Li[Li_{0.2}Mn_{0.13}Co_{0.13}]O_2$ [17], reportedly exhibit improved capacity and cycling stability after coating with graphene. Several reports detail about graphene-based $LiMn_2O_4$ materials. For example, Zhang et al. reported a facile method for preparing a nano-architectured lithium manganate/graphene hybrid to act as a positive electrode that could buffer the Jahn–Teller effect [18]. Jo et al. also reported a remarkable enhancement in the electrode performance of nanocrystalline $LiMn_2O_4$ after solvothermally assisted immobilisation on reduced graphene oxide nanosheets [19]. However, these graphene-based $LiMn_2O_4$ usually generate a hybrid or composite with graphene and $LiMn_2O_4$. Fewer reports describe coating spinel $LiMn_2O_4$ cathode materials with graphene in situ. Applying a graphene coating in situ may improve the electrochemical performance of spinel $LiMn_2O_4$.

However, graphene is generally prepared from graphite via exfoliation, and its two-dimensional sheet structure resists attempts to wrap the particle surface of the cathode materials tightly. Moreover, the manufacture procedure for graphene is complex and expensive, which limits further applications in LIB. Therefore, graphene-like coatings or quasi-graphenes have been developed and proposed for use in advanced LIB [20–22]. However, to our knowledge, spinel $LiMn_2O_4$ materials coated with graphene-like membranes in situ have not been disclosed. Due to the actions of carbon and graphene coatings mentioned above, the cathode materials containing spinel $LiMn_2O_4$ coated with graphene-like membranes in situ should exhibit improved discharge capacity and the capacity retention.

Recently, to improve LIB, we constructed a novel graphene-like membrane using liquid-polyacrylonitrile (LPAN) as the carbon source [23,24]. The membrane exhibits a carbon layer structure and electronic behaviours similar to graphene; this membrane may be prepared and modified easily. In this study, we hypothesised that the pristine $LiMn_2O_4$ particles could be coated with a very thin graphene-like layer in situ using LPAN as the carbon source. LPAN carbonisation on the particle surface forms an electrical network within the secondary particle. In this paper, we describe new findings regarding graphene-like coatings and their improvements on the electrochemical performance of spinel $LiMn_2O_4$ cathode materials that were determined through detailed structural analysis and electrochemical characterisations.

2. Experiment

2.1. Synthesis

Li_2CO_3 (98%, Aldrich) and MnO_2 (98%, Fluka) were used as the starting materials. The mixed compound was ground in a planetary ball mill in a 1:4 ratio of $n(Li_2CO_3)$:$n(MnO_2)$. The $LiMn_2O_4$ compounds were prepared using a solid-state ball milling method [25,26]. Afterwards, the 200 mesh $LiMn_2O_4$ compounds were mixed proportionally with LPAN and absolute ethanol. The mixed sample was ground again for 10 h at 400 r min^{-1}. The milled sample was dried in a 65 °C oven to evaporate the absolute ethanol before being dried at 220 °C for 3 h to sufficiently pre-oxidise the LPAN precursor. Finally, the pre-oxidised precursor was heated in air for 10 h at 750 °C in a muffle furnace; the final product was obtained after gradual cooling to room temperature.

2.2. Structure characterisation

The precursor's thermal decomposition behaviour was examined using thermo-gravimetric analysis (TGA). X-ray diffraction (XRD) experiments were performed on a D8 advance diffractometer (Bruker, Germany) equipped with a Cu target, an X-ray tube and a diffracted beam monochromator. The profile refinements of the collected data were conducted using the MDI Jade program. Raman spectra were measured with a Renishaw Invia Raman microscope (English) using non-polarised radiation at 514.5 nm. X-ray photoelectron spectroscopy (XPS) data were collected with an ESCALab220i-XL electron spectrometer from VG Scientific using 300 W AlKα radiation. The binding energies were referenced to the C1s line at 284.8 eV attributed to adventitious carbon. The XPS electron binding-energy scale was calibrated using the kinetic energy positions of the most prominent copper, silver, and gold photoemission lines. The experiments were performed in two connected ultrahigh vacuum (UHV) systems with base pressures of 5×10^{-10} mbar or better. The morphology of the powder samples was examined using Scanning Electron Microscopy (SEM, Hitachi, Japan) and high resolution transmission electron microscopy (HR-TEM).

2.3. Electrochemical characterisation

To prepare the electrodes, the powders were mixed with acetylene black and polyvinylidene difluoride powder (binder) at a ratio

of 80:10:10 in *N*-methyl-2-pyrrolidinone (NMP). After affixing the mixture to Al foil, the electrodes were dried: the NMP was removed at 80 °C over 2 h in air, and further drying occurred at 110 °C under vacuum for 6 h. The electrodes were tested in laboratory glass cells using Li metal foil as a counter electrode. The electrolyte contained 1 M $LiPF_6$ (Lithium hexafluorophosphate) in a 1:1 mixture (v/v) of DMC (dimethylcarbonate) and EC (ethylene carbonate). The assembly of the 2032 type coin cells was carried out in an Ar-filled glove box. The cells were discharged and charged at 25 °C at 14.8 mAh g^{-1} between 3.0 and 4.5 V. The galvanostatic charge–discharge test was conducted using a Land CT2001A testing system. The electrochemical measurements were performed using a SL1260 electrochemical station. The electrochemical impedance spectra (EIS) measurements were measured using a Solatron 1260 Impedance Analyser from 10^5 to 5 mHz. All experiments were conducted at room temperature.

3. Results and discussion

Before investigating the cathode materials, the precursor mixture of Li_2CO_3 and MnO_2 and the graphene-like membrane were first investigated using TGA, TEM, Raman and XRD. Fig. 1(a) presents the precursor's TGA–DTG curves. The precursor obviously displays three important weight losses. The initial endothermic peak (1) occurred from 100 to 200 °C, exhibiting a ca.8 wt% weight loss attributed to the adsorbed water. The second, sharper endothermic peak (2) appeared at 200–400 °C with a 8 wt% weight loss. This peak was attributed to the thermal decomposition of mixed carbonates. A considerable amount of CO_2 was continuously liberated during this stage. Finally, the third endothermic peak (3) occurred between 400 and 950 °C with a 2 wt% weight loss. This last stage weight loss was due to thermal decomposition of carbon (LPAN). Afterwards, only a small amount of weight was lost, and the TG curve became smooth and flat, indicating that a stable complex had formed above 400 °C. Consequently, to prepare a stable oxide containing mixed transition metals such as $LiMn_2O_4$, the precursor must be calcined above 400 °C. Therefore, the $LiMn_2O_4$ and the graphene-like membrane-coated $LiMn_2O_4$ were all treated above 400 °C during this experiment.

LPAN has been widely used to prepare carbon materials, including carbon nanotubes and fibres [27,28]. During this experiment, the LPAN was used to form a graphene-like coating. The morphology and structure of the graphene-like membrane was investigated first. Fig. 1(b)–(d) presents the HR-TEM images, Raman-spectra and XRD patterns for the graphene-like membrane calcined from LPAN. Fig. 1(b) reveals a very thin layer with graphene-like layer structure, as captured by the HR-TEM. In the Raman spectra (see Fig. 1(c)) of the graphene-like membrane from pure LPAN, there were two strong peaks at 1347 cm^{-1} and 1591 cm^{-1} and two weak peaks at 2694 cm^{-1} and 2950 cm^{-1}. These signals are characteristic peaks for carbon structures. Among these peaks, 1347 cm^{-1} was the D peak and was attributed to the first-order zone boundary phonons. G peak was at 1591 cm^{-1} and generated by in-plane optical vibrations; 2694 cm^{-1} is the 2D peak

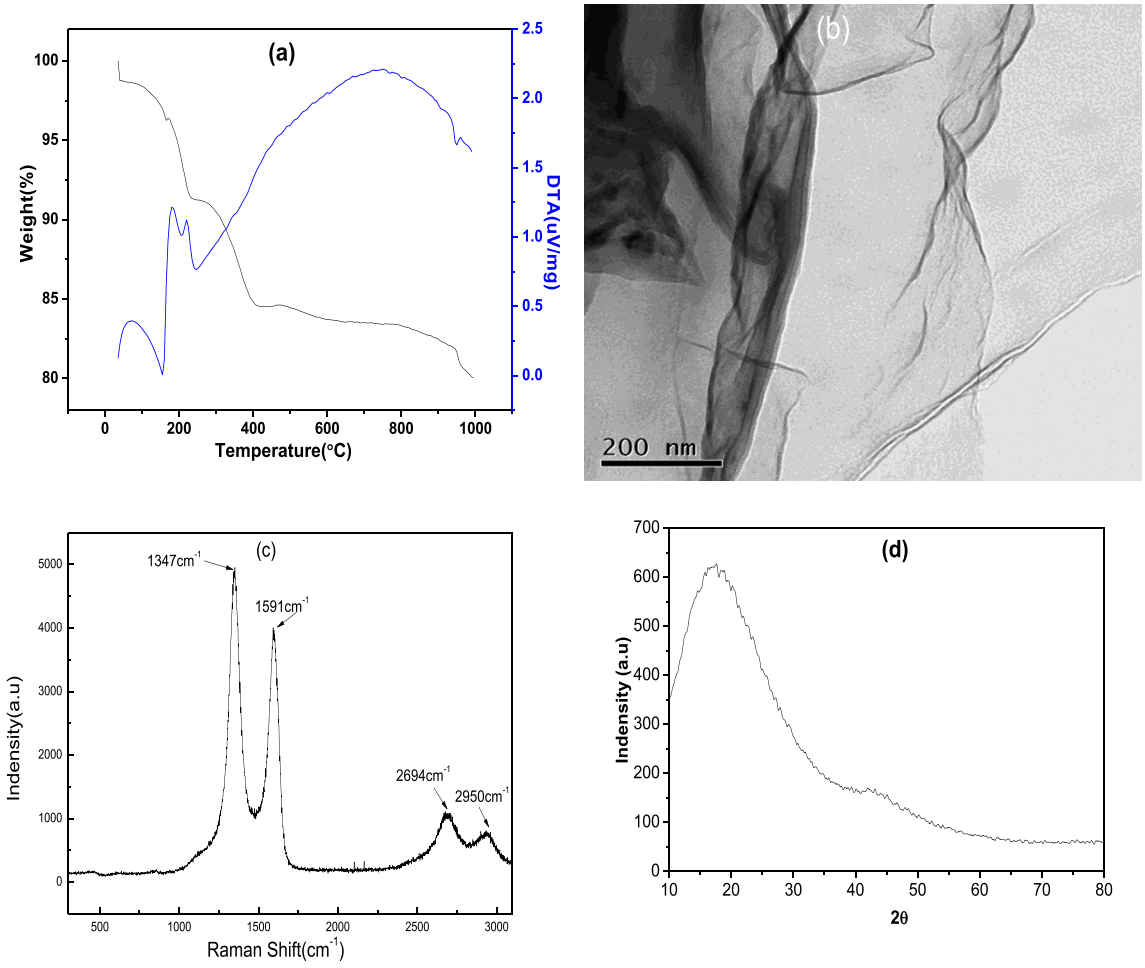

Fig. 1. (a) TGA–DTG curves of precursor; (b) HR-TEM image, (c) Raman-spectra, (d) XRD pattern for the graphene-like membrane calcined from pure LPAN.

caused by the second-order zone boundary phonons. This structure was very similar to that of graphene [29]. Moreover, the XRD of the graphene-like membrane also revealed its amorphous structure. Therefore, the graphene-like membrane was confirmed to have a typical graphene-like layered carbon structure that could be used to modify the surface of cathode materials, as discussed above.

According to the analysis of the precursor and the graphene-like membrane, the spinel $LiMn_2O_4$ cathode materials coated with the graphene-like membrane were prepared at different calcination temperatures and with different LPAN contents to optimise the preparation conditions and composition. The SEM images and XRD patterns for the 20 wt% LPAN-coated $LiMn_2O_4$ at different calcination temperature reveal that $LiMn_2O_4$ calcined at 750 °C forms the most stable and complete spinel crystal structure (see Supporting information Fig. A and Fig. B). Subsequently, the LPAN content was studied. Fig. 2 displays the XRD patterns of $LiMn_2O_4$ calcined at 750 °C coated in situ with graphene-like membranes with various LPAN contents. All of the diffraction peaks corresponded to a spinel structure and agreed with those of the standard spinel $LiMn_2O_4$ (PDF: 35-0782). Though the relative XRD intensities in the $LiMn_2O_4$ sintered with the 30 wt% LPAN were much stronger, the XRD patterns of the powders sintered with different LPAN content were similar to those of the pure spinel $LiMn_2O_4$. Therefore, the graphene-like membrane and the LPAN content did not influence the spinel structure formation in $LiMn_2O_4$, possibly because the graphene-like coating was an amorphous carbon structure formed only on the particles' surfaces. This structure should differ from the previous graphene–$LiMn_2O_4$ composites or hybrids [18].

The graphene-like membrane coating and its influence may be assessed further using the XPS spectra. Fig. 3 provides the XPS data for the $LiMn_2O_4$ calcined at 750 °C coated with a graphene-like membrane with various LPAN contents. The fitting curves from the C1s spectrum are provided in the supporting information (see Supporting information Fig. C). In this experiment, all XPS spectra were measured using powder affixed to double-sided adhesive tape. Consequently, the C1s peaks for the double-sided adhesive tape were also measured in all samples. In the pure $LiMn_2O_4$, a peak at approximately 292 eV was attributed to the O 1s binding energy, while the C1s of C–O bond tended to appear above 288 eV. These peaks should be from the double-sided adhesive tape. In addition to these peaks, a new C 1s peak appeared at approximately 287.4–287.6 eV in the 20 wt% LPAN-coated and 30 wt% LPAN-coated $LiMn_2O_4$ (see Supporting information Fig. C). This new peak should be from the LPAN-derived graphene-like membrane because the binding energy of the C 1s for the C–C in a graphene-like membrane is generally lower than that for the C–O. Moreover, the peak intensities in the C 1s spectrum increased with the LPAN content. In contrast, the peak intensities in the Mn 2p3 spectrum decreased with the LPAN content due to the increased amount of coating or LPAN content; the binding energy of Mn 2p3 remained unchanged. Therefore, the graphene-like membrane was confirmed to have formed only on the surface of particles and did not disrupt the original structure.

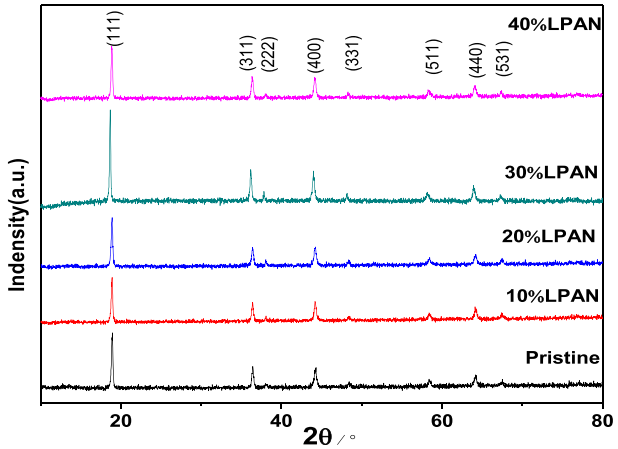

Fig. 2. XRD patterns of $LiMn_2O_4$ calcined at 750 °C coated in situ with graphene-like membranes with various LPAN contents compared to the pristine.

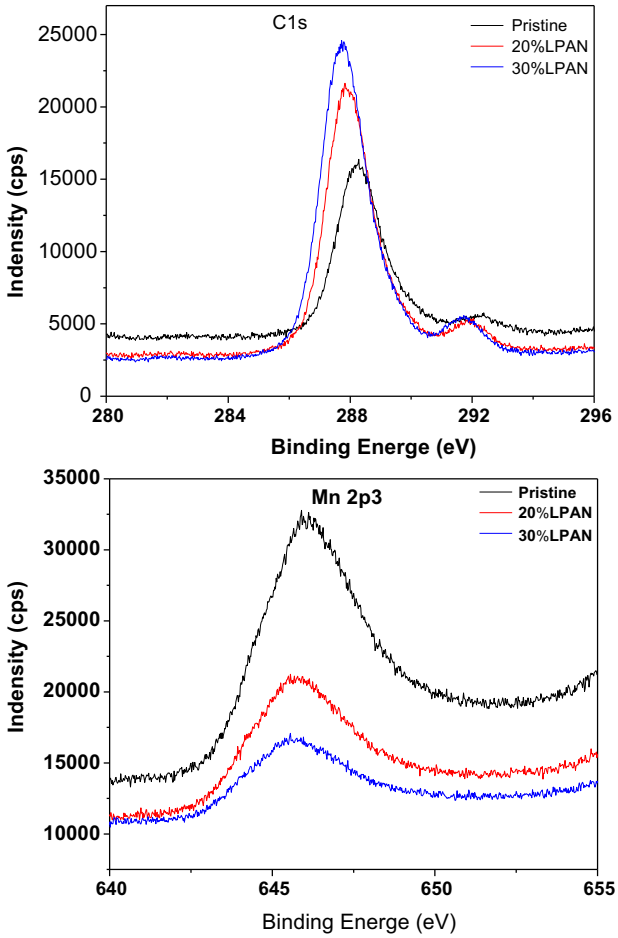

Fig. 3. XPS data for the $LiMn_2O_4$ calcined at 750 °C coated with a graphene-like membrane with various LPAN contents compared to the pristine.

The morphology of the $LiMn_2O_4$ coated with a graphene-like membrane was investigated using SEM and EDS. The SEM images of $LiMn_2O_4$ calcined using 20 wt% LPAN at different temperatures are provided in Supporting information. The SEM images of $LiMn_2O_4$ calcined from 20 wt% LPAN at different temperatures indicate that high calcination temperatures significantly improved the particle size (see Supporting information Fig. B). However, the high temperature calcination generated some unnecessary crystalline structures. Therefore, the optimal calcination temperature was 750 °C. During this experiment, we mainly studied the morphology of $LiMn_2O_4$ coated with the graphene-like membrane in situ and calcined at 750 °C. Fig. 4(a)–(d) presents the SEM images for the $LiMn_2O_4$ coated with the graphene-like membrane in situ and calcined at 750 °C with various LPAN contents. The $LiMn_2O_4$ morphology becomes increasingly uniform and the particle size grows as the LPAN content increases. Therefore, the graphene-like membrane facilitates the spinel $LiMn_2O_4$ particle growth, possibly because the LPAN improves the agglomeration of particles before the calcination, forming larger particles during the heat treatment.

The graphene-like membrane was difficult to detect in the SEM image, possibly because it coated the $LiMn_2O_4$ surface. In the EDS image (see Fig. 4(e)), there was a C element in addition to the Li, Mn and O signals. Therefore, the LPAN formed a layered carbon structure during the calcination step, and the carbon layer exists as part of the $LiMn_2O_4$ morphology.

TEM is a good method to assess the coating of particles in situ. Fig. 5 reveals the HR-TEM images for the $LiMn_2O_4$ coated with graphene-like membrane (20 wt% LPAN) calcined at 750 °C. The layers were ca.3 nm thick and coated onto the bare $LiMn_2O_4$ surface (see Fig. 5(c)). The coated sample was crystalline, with lattice fringes extending to the grain boundary. For instance, the distances between the neighbouring lattice fringes were approximately 0.476 nm and 0.249 nm, corresponding corresponds to the d-spacing of the (111) and (311) planes, respectively, in the Li–Mn–O spinel phase. The electron diffraction pattern also reveals that there are clear crystalline spinel $LiMn_2O_4$ lattices under the coating (see Fig. 5(d)). These crystal lattices agreed with the XRD pattern discussed above. The as-prepared graphene-like membrane was successfully coated on the spinel $LiMn_2O_4$ surface in situ. This graphene-like membrane-coated spinel $LiMn_2O_4$ cathode material may exhibit improved electrochemistry performance.

The electrochemical properties of the graphene-like membrane-coated spinel $LiMn_2O_4$ were systematically investigated using their charge/discharge capacity and cycling stability. Fig. 6(a) displays the initial charge–discharge curves for the LIB cells cycled at 0.1 C between 3.0 and 4.4 V, and their discharge capacities as a function of their cycle numbers are presented in Fig. 6(b). The cycling stability curves for $LiMn_2O_4$ with different proportions of LPAN calcined at different temperatures are also provided in the supporting information (see Supporting information Fig. D). From the cycling stability curves of the $LiMn_2O_4$ calcined at different temperatures, the cathode materials calcined at 750 °C demonstrated the best electrochemical properties (see Supporting information

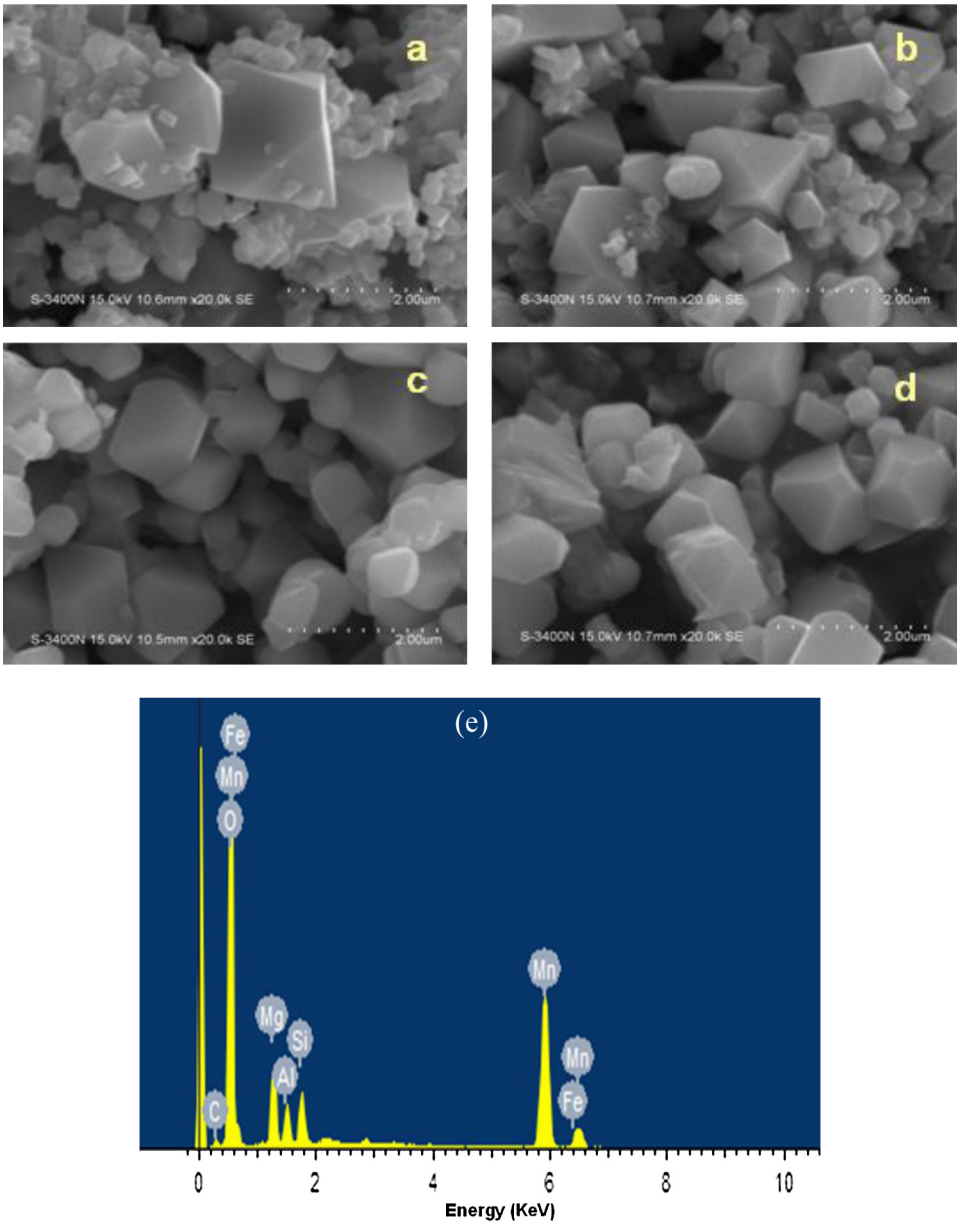

Fig. 4. (a–d) SEM images for the $LiMn_2O_4$ coated with the graphene-like membrane in situ and calcined at 750 °C with various LPAN contents (a – 10 wt%; b – 20 wt%; c – 30 wt%; d – 40 wt%); (e) EDS of 20 wt% LPAN-coated $LiMn_2O_4$.

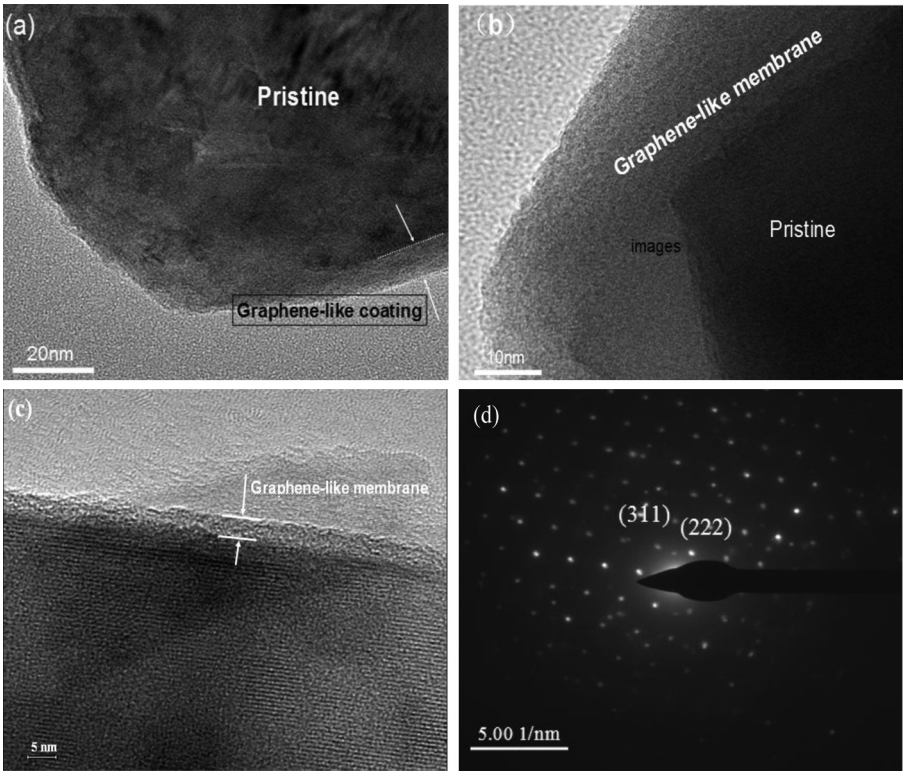

Fig. 5. HR-TEM images (a–c) and electron diffraction pattern (d) for the $LiMn_2O_4$ coated with graphene-like membrane (20 wt% LPAN) calcined at 750 °C.

Fig. D). In addition, Fig. 6(a) indicates that all cells made from material calcined at 750 °C exhibited charge and discharge profiles similar to pure $LiMn_2O_4$. Both the charge and discharge curves exhibited two pseudoplateaus at approximately 4.0 and 4.1 V. This electrochemical behaviour is typical of spinel $LiMn_2O_4$ and indicates that the insertion and extraction of Li^+ occurs in two stages. The voltage plateau at approximately 4.0 V arose from the Li^+ removal from half of the tetrahedral sites where Li–Li interactions occur. The second voltage plateau appeared at approximately 4.1 V and was attributed to the removal of Li^+ from the tetrahedral sites without Li–Li interactions [12]. Therefore, the graphene-like membrane did not influence the charge–discharge process, nor did it prevent the insertion and desertion of Li^+. In addition, Fig. 6(b) reveals that the cathode material made of spinel $LiMn_2O_4$ coated with a graphene-like membrane in situ demonstrate improved discharge capacity and better cyclability relative to the pure spinel $LiMn_2O_4$. In particular, when the LPAN content was increased to 20 wt%, good discharge capacity and cyclability were obtained. The first discharge capacity was 131.1 mAh g^{-1}, and the capacity was 125.3 mAh g^{-1} after 50 cycles, retaining 96% of the original values. When the LPAN content was 40 wt%, the first discharge capacity as increased to above 132 mAh g^{-1}, but the cycle retention was decreased after 30cycles. Furthermore, the C-rate dependence of the discharge capacity (see Supporting information Fig. F) also indicated that the 20 wt% LPAN graphene-like membrane displayed a better C-rate discharge capacity. The 20 wt% LPAN-coated graphene-like membrane did not exhibit a higher discharge capacity, but the electrochemical performance reveal that coating spinel $LiMn_2O_4$ with a graphene-like membrane in situ improved the discharge capacity and cycling stability of a LIB significantly.

To understand the effect of the graphene-like membrane on the coated spinel $LiMn_2O_4$ cathode materials, cyclic voltammetry tests were conducted on both the pure and graphene-like membrane-coated spinel $LiMn_2O_4$ cathode materials at 0.2 mV s^{-1} from 3.0 to 4.4 V at 25 °C. Fig. 7 displays the CV curves for the 20 wt% LPAN-coated $LiMn_2O_4$ alongside the pure $LiMn_2O_4$ between 3.0 and 4.4 V. Both the pure and graphene-like membrane-coated $LiMn_2O_4$ cathode materials exhibited similar charge and discharge profiles. During the charging process, two oxidation peaks were observed in the CV curves. The first peak appeared at 4.1 V, revealing the change from $LiMn_2O_4$ to $Li_{0.5}Mn_2O_4$; the second peak appeared at 4.2 V, corresponding to the change from $Li_{0.5}Mn_2O_4$ to Mn_2O_4. However, during the discharge process, there were also two reduction peaks. The first peak appeared at 4.08 V and the second peak appeared at 3.91 V. These peaks were attributed to the changes from Mn_2O_4 to $Li_{0.5}Mn_2O_4$, and from $Li_{0.5}Mn_2O_4$ to $LiMn_2O_4$, respectively. This process was consistent with the known mechanism for the electrochemical insertion/extraction of Li in $LiMn_2O_4$ cathode materials [11]. These data confirmed that the graphene-like membrane did not influence the insertion or desertion of Li^+. However, the current density improved significantly for the graphene-like membrane-coated $LiMn_2O_4$ cathode materials relative to the pure $LiMn_2O_4$ cathode materials. Therefore, the graphene-like membrane facilitated the electron movement, similar to the carbon coatings mentioned above. The coating improved the charge–discharge capacity, as discussed above, and was consistent with the initial charge–discharge analysis.

Fig. 8 reveals the EIS of the graphene-like membrane-coated $LiMn_2O_4$ materials with various LPAN contents. Compared to the pure $LiMn_2O_4$, the graphene-like membrane-coated $LiMn_2O_4$ exhibited a smaller charge transfer resistance (R_{ct}), while the R_{ct} increased slightly during the insertion and extraction of Li^+. The R_{ct} might have increased because the graphene-like membrane favours the alleviation of manganese dissolution and the precipitation of resistive components, such as LiF and MnF_2; these resistive components arose from decomposed $LiPF_6$ electrolyte and the $LiMn_2O_4$ corroded by HF during cycling [30]. The smaller R_{ct} favoured the

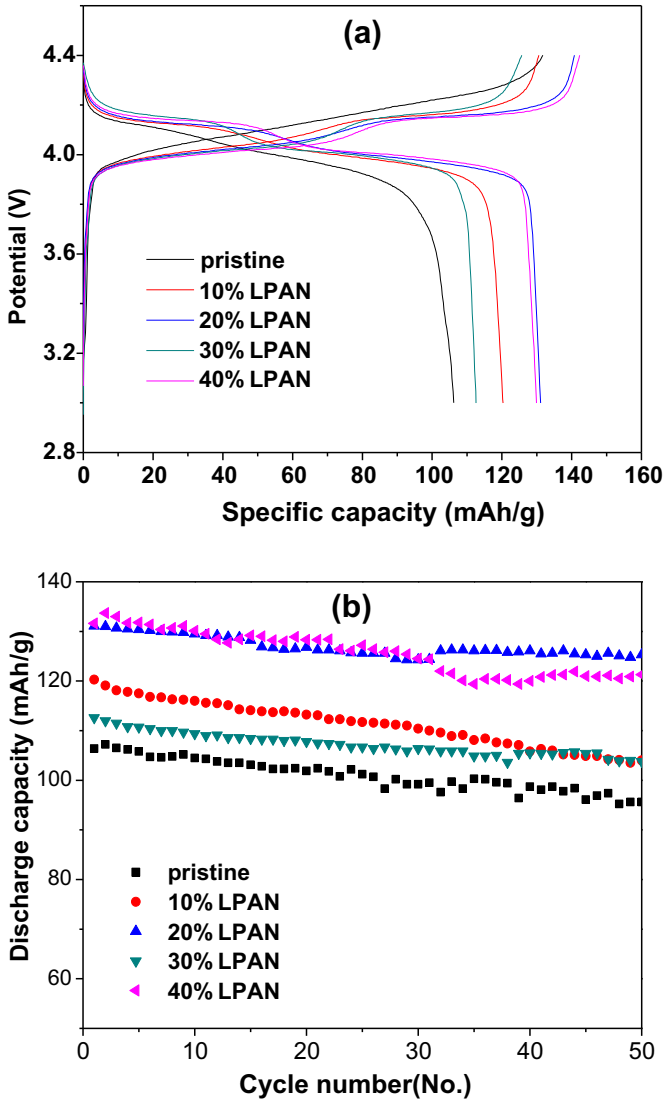

Fig. 6. Initial charge–discharge curves (a) and cycling stability curves (b) for the LIB cells made from the $LiMn_2O_4$ in-situ coated with graphene-like membrane compared to the pristine.

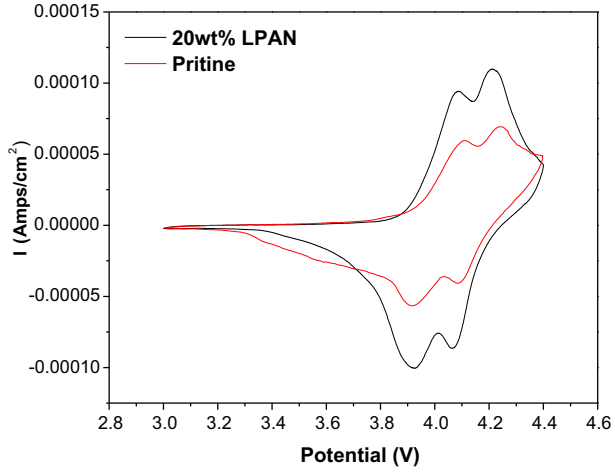

Fig. 7. CV curves of 20 wt% LPAN-coated $LiMn_2O_4$ compared to the pristine between 3.0 V and 4.4 V.

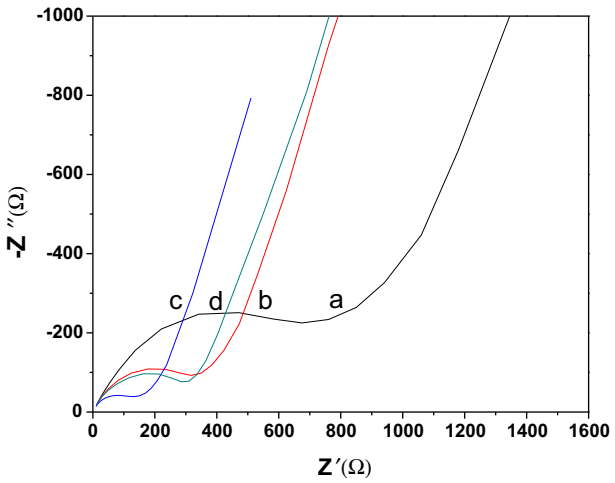

Fig. 8. EIS of the graphene-like membrane-coated $LiMn_2O_4$ materials with various LPAN contents (a – 0 wt%, b – 10 wt%, c – 20 wt%, d – 30 wt%).

rapid electrochemical reactions and might improve the electrochemical performance of the active materials. In particular, because the smallest R_{ct} was measured for the 20 wt% LPAN-coated $LiMn_2O_4$, those cathode materials exhibited better electrochemical performance than the pure $LiMn_2O_4$. This result was validated by the capacity and stability analyses discussed above. However, the R_{ct} grew when the LPAN content increased to 30 wt%. Therefore, excess LPAN might thicken the coating layer, hindering the Li^+ migration. Therefore, adding the graphene-like membrane improved the electrochemical performance of spinel $LiMn_2O_4$ cathode materials.

4. Conclusions

A novel spinel $LiMn_2O_4$ coated with a graphene-like membrane in situ was prepared using LPAN as the carbon source. The structure and electrochemical performance of the graphene-like membrane-coated spinel $LiMn_2O_4$ was systematically investigated. The graphene-like membrane had a typical graphene-like layered carbon structure that could be generated in situ on the surface of $LiMn_2O_4$ particles without affecting their crystal structure. Moreover, the graphene-like membrane helps increase the particle size. The electrochemical performance also revealed that the graphene-like membrane significantly improved the discharge capacity and cycling stability of spinel $LiMn_2O_4$. In particular, the coated $LiMn_2O_4$ with 20 wt% LPAN reached 131.1 mAh g^{-1} at room temperature, while up to 96% of the capacity was retained after 50 cycles at 0.1 C. The CV and EIS analyses also demonstrated that the graphene-like membrane did not influence the insertion or desertion of Li^+. The improved electrochemical performance of the graphene-like membrane-coated $LiMn_2O_4$ was attributed to the decreased amount of manganese dissolved in the electrolyte and the smaller charge transfer resistance generated by the graphene-like membrane coating.

Acknowledgements

The authors are highly grateful for the financial support from China Postdoctoral Science Foundation funded project (Grant No. 2012M521624), National Natural Science Foundation of China (Grant No. 21001074, 21004040 and 21104045), Specialized Research Fund For The New Energy Industrial Development of Shenzhen and The Foundation Research Plan Major Cultivation Project of Shenzhen (Grant No. JC201104210008A). We are grateful to Prof. Chen Shaojun for helping us to get the micro-Raman

data and XPS data. The TEM used in this work was supported by the Institute for Advanced Materials (IAM) with funding from the Special Equipment Grant from the University Grants Committee of the Hong Kong Special Administrative Region, China (SEG_HKBU06).

Appendix A. Supplementary data

Supplementary data related to this article can be found at http://dx.doi.org/10.1016/j.jpowsour.2013.09.007.

References

[1] T.F. Yi, Y.R. Zhu, X.D. Zhu, J. Shu, C.B. Yue, A.N. Zhou, Ionics 15 (2009) 779.
[2] T. Yi, C. Yue, Y. Zhu, R. Zhu, X. Hu, Rare Met. Mater. Eng. 38 (2009) 1687.
[3] Z.S. Zheng, Z.L. Tang, Z.T. Zhang, W.C. Shen, J. Inorg. Mater. 18 (2003) 257.
[4] C. Qinghua, C. Haiyun, Z. Shengli, W.E.N. Jiuba, Q.I.N. Qizong, Chem. World 49 (2008) 749.
[5] P. Cheng, X. Lai, Y.H. Li, C.Y. Wu, B. Li, D.J. Gao, J. Bi, Mater. Rev. 22 (2008) 104.
[6] L.J. Fu, H. Liu, C. Li, Y.P. Wu, E. Rahm, R. Holze, H.Q. Wu, Solid State Sci. 8 (2006) 113.
[7] J.D. Han, S. Jin, Y. Jing, W. Li, Y.Z. Jia, Chin. J. Inorg. Chem. 21 (2005) 237.
[8] A.R. Han, T.W. Kim, D.H. Park, S.-J. Hwang, J.H. Choy, J. Phys. Chem. C 111 (2007) 11347.
[9] A. Bhaskar, M. Deepa, T.N. Rao, U.V. Varadaraju, J. Electrochem. Soc. 159 (2012) A1954.
[10] M. Tang, A. Yuan, H. Zhao, J. Xu, J. Power Sources 235 (2013) 5–13.
[11] S. Parvathy, R. Ranjusha, K. Sujith, K.R.V. Subramanian, N. Sivakumar, S.V. Nair, A. Balakrishnan, J. Nanomater. 2012 (2012) 259684.
[12] Q.C. Zhuang, T. Wei, L.L. Du, Y.L. Cui, L. Fang, S.G. Sun, J. Phys. Chem. C 114 (2010) 8614.
[13] J.K. Kim, J.W. Choi, G.S. Chauhan, J.H. Ahn, G.C. Hwang, J.B. Choi, H.J. Ahn, Electrochim. Acta 53 (2008) 8258.
[14] Z. Qin, X. Zhou, Y. Xia, C. Tang, Z. Liu, J. Mater. Chem. 22 (2013) 21144.
[15] L. Zhang, S. Wang, D. Cai, P. Lian, X. Zhu, W. Yang, H. Wang, Electrochim. Acta 91 (2013) 108.
[16] Y. Zhang, W. Wang, P. Li, Y. Fu, X. Ma, J. Power Sources 210 (2012) 47.
[17] Z. He, Z. Wang, H. Guo, X. Li, X. Wu, P. Yue, J. Wang, Mater. Lett. 91 (2013) 261.
[18] W. Zhang, Y. Zeng, C. Xu, N. Xiao, Y. Gao, L.-J. Li, X. Chen, H.H. Hng, Q. Yan, Beilstein J. Nanotechnol. 3 (2012) 513.
[19] K.Y. Jo, S.Y. Han, J.M. Lee, I.Y. Kim, S. Nahm, J.W. Choi, S.J. Hwang, Electrochim. Acta 92 (2013) 188.
[20] G. Ma, H. Peng, J. Mu, H. Huang, X. Zhou, Z. Lei, J. Power Sources 229 (2013) 72.
[21] Y. Liu, L. Jiao, Q. Wu, J. Du, Y. Zhao, Y. Si, Y. Wang, H. Yuan, J. Mater. Chem. A 1 (2013) 5822.
[22] Q. Peng, X.J. Chen, S. Liu, S. De, RSC Adv. 3 (2013) 7083.
[23] J.H. Liu, D.Y. Gui, Q.L. Zhang, C.X. He, C.Z. Zhu, PCT Patent 2012/089085, 2012.
[24] J.H. Liu, J. Xu, Q.L. Zhang, C.X. He, C.Z. Zhu, CN 201110086492.7, 2011.
[25] D.D.M. Zhonghua Lu, J.R. Dahn, Electrochem. Solid-State Lett. 4 (2001) A191.
[26] Z.H. Lu, J.R. Dahn, J. Electrochem. Soc. 148 (2001) A237.
[27] Q. Yang, G. Sui, Y.Z. Shi, S. Duan, J.Q. Bao, Q. Cai, X.P. Yang, Carbon 56 (2013) 288.
[28] K.E. Perepelkin, Fibre Chem. 34 (2002) 271.
[29] Z. Ni, Y. Wang, T. Yu, Z. Shen, Nano. Res. 1 (2008) 273.
[30] H.B. Sun, D. Zhu, Y.G. Chen, C.H. Xu, L.H. Huang, H. Yang, J. Solid State Electrochem. 16 (2012) 2979.